

Mechanisms of polycyclic aromatic hydrocarbons formation in flames

Gerasimov G. Ya.

Institute of Mechanics, M. V. Lomonosov Moscow State University

1 Michurinsky Ave., Moscow, 119192, Russia

Abstract

The analysis of the existing mechanisms of polycyclic aromatic hydrocarbons formation in hydrocarbon flames was performed. It was shown that the growth of aromatic molecules includes both the addition of acetylene molecules with subsequent rearrangement of new aromatic structure and coagulation, in which higher aromatic molecules are assembled from different aromatic fragments. The recommended optimal mechanism of aromatic compounds formation includes the irreversible *zipper* variety of the coagulation mechanism that begins to work, when the number of C-atoms in the formed aromatic particle exceeds 20.

1. Introduction

The investigation of polycyclic aromatic hydrocarbons (PAHs) and soot formation under combustion is one of the main directions in the combustion chemistry. The interest in the problem is particularly determined by the ecological requirements to liquid-fuel rocket motors that use hydrocarbon fuels such as kerosene. According to these requirements the emission of harmful substances into the atmosphere should comply with adopted standards. PAHs and soot particles (black carbon) warm the atmosphere directly by absorbing sunlight and indirectly by affecting cloud formation. Most other atmospheric particles, such as sulphates, primarily scatter sunlight and cause global cooling. Several recent calculations conclude that the radiative forcing due to black carbon is $0.5 - 0.8 \text{ W/m}^2$, which is one-half of the forcing due to CO_2 (1.46 W/m^2), and is larger than the forcing from the second most important greenhouse gas (CH_4) [1].

Harmful admixtures formed at rocket flights in the atmosphere are the only immediate anthropogenic pollutants at high altitudes. The trajectory of the rocket motion is characterized by very high harmful substances concentrations including PAHs and soot particles and energy contributions. It is possible in such conditions the beginning of “trigger” mechanisms, which may call into action chain reactions with much more response than primary influence [2]. The use of chlorine-containing fuels in solid-fuel rocket motors leads to sudden injection of atomic or molecular chlorine into the stratosphere that cause a prompt local depletion of ozone, which will persist until ozone-rich air is mixed into the depleted region by the diffusion [3].

The construction of kinetic mechanisms for complex chemically reacting systems usually includes comparison of model calculations with experimental data. At the present time, there is a large number of experimental information suitable for testing kinetic models of the formation of higher PAHs and soot at combustion of aliphatic and aromatic hydrocarbons (see, for example, [4]). This information includes the concentration and temperature profiles obtained with the use of the GC-MS and MB-MS methods of analysis of the corresponding flames.

Multiple experimental data show that the formation and further modification of PAHs structure under combustion of hydrocarbon fuels is a complex multistage process closely connected with the general kinetic mechanism of combustion [5]. The kinetic scheme of the process includes the following main stages: 1) combustion of the initial fuel; 2) formation of larger hydrocarbon molecules and radicals and, finally, of small aromatic molecules; 3) growth of aromatic molecules due to the addition to them of acetylene molecules (so-called HACA-mechanism); 4) coagulation of PAHs molecules and radicals; 5) ion-molecular reactions.

Despite the simplicity of the scheme of PAHs molecules formation, the structure of all stages of the process and the role of individual elementary reactions are still not clearly understood. The aim of the present work is to analyze the existing mechanisms of higher PAHs formation and to choose the most optimal kinetic model giving the best agreement with available experimental data.

2. Description of the kinetic model

The general kinetic model of PAHs formation includes both the combustion kinetics with formation of single-ring aromatics and the sequential growth of PAHs molecules up to formation of soot particles in reactions with stable and radical species. The most important intermediate combustion product from the point of view of PAHs molecules growth is acetylene molecules, which formed due to the high-temperature oxidation of any hydrocarbon fuels.

2.1 Combustion of initial fuel

The first group of reactions in the general kinetic model of PAHs formation is responsible for the combustion process. This group is determined by the composition of the initial fuel and can be represented by kinetic models of different degrees of detailing. Liquid hydrocarbon rocket fuel (kerosene) consists of aliphatic saturated (paraffins), alicyclic (naphthenes), and aromatic (arenes) hydrocarbons. Typical representatives of linear paraffins in kerosene are *n*-dodecane ($n\text{-C}_{12}\text{H}_{26}$) and *n*-tetradecane ($n\text{-C}_{14}\text{H}_{30}$). Paraffins with a branched chain are represented mainly by *iso*-octane ($i\text{-C}_8\text{H}_{18}$). Naphthenes are present predominantly in the form of monocyclic compounds, such as cyclohexane ($\text{cy-C}_6\text{H}_{11}$) and methyl cyclohexane ($\text{CH}_3\text{cy-C}_6\text{H}_{11}$). The content of arenes in kerosene is limited in connection with their increased tendency toward carbonization. The highest concentrations among them have toluene ($\text{CH}_3\text{-C}_6\text{H}_5$) and ethyl benzene ($\text{C}_2\text{H}_5\text{-C}_6\text{H}_5$) [6].

Detailed kinetic models of combustion of aliphatic saturated hydrocarbons with a normal and branched chain are currently at the stage of development of the kinetic mechanism structure for molecules of the starting fuel with a number of C atoms of about 10 or higher and at the stage of refinement of the corresponding rate constants of the reactions. These models include the kinetic mechanisms of combustion in $\text{H}_2/\text{O}_2/\text{CO}$, C_1/C_2 , and C_3/C_4 subsystems. The rate constants of the elementary reactions describing the behavior of these systems are based on the results of their direct measurements and have a fairly high degree of reliability. The basic classes of reactions for high-temperature oxidation of paraffines are [7]:

- (a) *unimolecular decomposition of fuel* (initiating stage) with formation of two alkyl radicals or a heptyl radical and atom H;
- (b) *H-atom abstraction from a fuel molecule* in its interaction with atoms and radicals, which leads to the formation of heptyl radicals;
- (c) *alkyl radical β -scission* with formation of olefin molecule and smaller alkyl radical;
- (d) *interaction of the alkyl radical with the oxygen molecule* followed by decomposition of the adduct formed into olefin and an HO_2 radical.

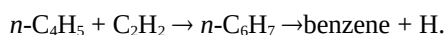
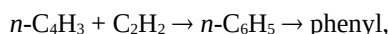
Branching of the chain in high-temperature oxidation occurs in the reaction $\text{H} + \text{O}_2 \rightarrow \text{OH} + \text{O}$. The content of naphthene hydrocarbons in gasoline can attain 80%. Whereas the combustion of aliphatic hydrocarbons has been studied with a sufficient degree of details, the combustion of naphthenes has received much less attention. The mechanism of cyclohexane combustion is quite simple as compared to the corresponding mechanism for higher aliphatic compounds due to high symmetry of its molecule. Only one cyclohexyl radical can actually be formed at H-atom abstraction from the starting fuel molecule. The reaction of β -decomposition of the cyclohexyl radical at high temperatures opens the ring and forms a linear hexenyl radical. A simplified (quasiglobal) kinetic mechanism of high-temperature oxidation of cyclohexane has been prepared in [8]. The decomposition products are further oxidized in accordance with a detailed kinetic mechanism.

The concentration of aromatic hydrocarbons in kerosene is no higher than 22%, and for certain types of kerosene this quantity amounts to only several per cent of the total mass of the fuel. Therefore, the kinetics of oxidation of these fuel components does not exert a strong influence on the general dynamics of the chemical process. Arenes are presented in kerosene mainly by toluene and ethyl benzene. The kinetic schemes of oxidation of these components are closely related to the kinetic schemes of oxidation of benzene [9]. The high-temperature oxidation of benzene is initiated by the breaking of the C-H bond in interaction

of benzene molecule with H and O atoms and OH radicals with formation of phenyl radical C_6H_5 . The basic channel of further transformation of this radical is its decomposition with breaking of the ring structure and formation of $n-C_4H_3$ radical and acetylene molecule.

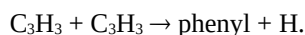
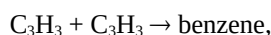
2.2 Formation of single-ring aromatic molecules

The formation of the first aromatic ring in the chemical reacting system that contain products of the thermal decomposition of initial hydrocarbon fuel is associated mainly with radicals $n-C_6H_5$ and $n-C_6H_7$, which are produced in reactions [10]:



Cyclization of these radicals occurs under the interaction of unpaired electron with triple bond between C-atoms in appropriate radical.

The second most important cyclization reaction channel in hydrocarbon flames is recombination of propargyl radicals [11]:



Because this reaction channel requires extensive internal rearrangements steps before nonaromatic adduct can isomerizes to hot benzene molecule and subsequently be stabilized or dissociate to phenyl and H-atom, these reactions are not elementary steps at high temperatures [10].

2.3 HACA-mechanism of aromatics growth

The further growth of PAHs molecules A_n , where n is the number of C-atoms in aromatic particle, is associated with the interaction of aromatic radicals with acetylene molecules. The process is described by the so-called HACA-mechanism (H-abstraction- C_2H_2 -addition) that consists of two principal reaction sequences [12]:

(a) abstraction of a hydrogen atom from the reacting aromatic molecule A_n under its interaction with gaseous hydrogen atom with the formation of aromatic radical R_n , $A_n + H \rightarrow R_n + H_2$,

(b) addition of gaseous acetylene molecule to the aromatic radical R_n , $R_n + C_2H_2 \rightarrow \text{products}$. Destruction of aromatic molecules and radicals occurs under their interaction with O atoms and O_2 molecules, respectively.

This mechanism, on the one hand, is a simplification of the total kinetic mechanism of growth of the aromatic structure of PAHs molecules. On the other hand, it represents fairly exactly the main steps of the formation of higher aromatic rings.

2.4 Coagulation of aromatic molecules and radicals

The coagulation mechanism describes the interaction between two PAHs particles (molecule/radical + radical) with the formation of a PAH dimer (C-C bond between two particles) followed by dehydrogenation of the dimer and closing of the ring. On the basis of the structural similarity of PAHs particles for the rate constants of reactions the corresponding values for reactions benzene + phenyl and phenyl + phenyl were chosen as standard ones [13]. Since the activation energies for these types of reactions are approximately equal, the pre-exponential factors in the rate constants were corrected towards higher values in accordance with the increase in the frequency of collisions $\nu \sim d_n^2(8\pi RT/\mu)^{1/2}$ for heavier PAHs particles than benzene [14]. Here d_n is diameter of the molecule with n C-atoms and μ is reduced mass of two colliding gas particles. If for the relation d_n/d_6 the expression $d_n/d_6 \approx 0.816 n^{1/2} - 1$ is taken, then the correction factor f_{mn} for the coagulation rate constant of two heavy PAHs particles can be written in the form:

$$f_{mn} = [0.408(m^{1/2} + n^{1/2}) - 1]^2 [12/(m + n)]^{1/2}.$$

In contrast to the general coagulation mechanism of aromatics growth, the bimolecular interaction of two PAHs particles in the so-called *zipper*-mechanism is accompanied by the abstraction from their periphery of several hydrogen atoms. In this case, several C–C bonds and the corresponding number of pentagonal and hexagonal cells are formed simultaneously [5]. The growth of aromatic molecules in this kind of the coagulation process has irreversible character.

In estimating the kinetic parameters of the *zipper*-mechanism, it is necessary to take into account that with increasing mass of PAHs radicals the difference in their behavior, as compared to the behavior of molecules of the same structure, disappears [15]. While for the pairs phenyl/benzene and naphthyl/naphthalene a much lower concentration of radicals and its later maximum are observed, the concentration curves of large PAHs radicals practically do not differ from the corresponding curves for PAHs molecules. Therefore, it may be suggested that the differences in reactivity between large PAHs radicals and molecules of equal structure at high temperatures are also insignificant.

2.5 Ion-molecular reactions

An important role in the formation of higher PAHs molecules can be played by ion-molecular reactions [16]. Charged components are formed practically in all hydrocarbon flames with the concentration of aromatic ions being about four orders of magnitude lower than the concentration of neutral PAHs of the same structure. The appearance of charged components in the flames is associated in the first place with the chemiionization reaction: $\text{CH} + \text{O} \rightarrow \text{CHO}^+ + \text{e}$ followed by charge exchange of CHO^+ on water molecules: $\text{CHO}^+ + \text{H}_2\text{O} \rightarrow \text{H}_3\text{O}^+ + \text{CO}$. The formation of positively charged ions PAH^+ occurs as a result of the charge exchange of H_3O^+ on PAHs molecules.

The further behavior of aromatic PAH^+ ions is only generally understood because of the lack of kinetic formation. The main channel of growth of the structure of PAH^+ is the reaction of addition of C_2H_2 to the aromatic radical with a rate constant exceeding by two orders of magnitude the corresponding value for the addition of C_2H_2 to the PAHs radical. Kinetic data on the coagulation of PAHs ions and molecules are practically absent. The rate constant of the dimerization reaction of C_6H_6^+ and C_6H_6 measured at temperatures close to room temperature and $p = 0.1$ Pa [17] is about two orders of magnitude lower than the corresponding value for the dimerization of phenyl radicals [13].

The Table shows the simplified kinetic model of the growth of PAHs particles in hydrocarbon flames chosen for numerical simulation that includes the above-described kinetic mechanisms. The model was corrected in performing calculations on the basis of comparison of the obtained results with the available experimental data. A detailed description of the changes made with corresponding comments is given below.

Table: Kinetic model of PAHs structure growth in hydrocarbon fuels

Reaction	lgA	E/R, K	References
HACA-mechanism			5
$A_n + \text{H} \rightarrow R_n + \text{H}_2$	14.40	8050	[5]
$R_n + \text{H}_2 \rightarrow A_n + \text{H}$	12.60	3970	[18]
$R_n + \text{C}_2\text{H}_2 \rightarrow A_{n+2} + \text{H}$	13.60	5080	[5]
$R_n + \text{C}_2\text{H}_2 \rightarrow R_{n+2}$	13.60	5080	[5]

$R_n + O_2 \rightarrow A_{n-2} + HCO + CO$	12.32	3760	[10]
$R_n + H \rightarrow A_n$	14.34	-	[19]
Coagulation mechanism			
$R_m + R_n \rightarrow A_{m+n}$	13.14	56	[13]
$R_m + A_n \rightarrow A_{m+n} + H$	11.98	2170	[13]
$A_{m+n} + H \rightarrow R_m + A_n$	13.61	4420	[13]
Ion-molecular mechanism			
$H_3O^+ + A_n \rightarrow R_n^+ + H_2O$	14.90	-	[16]
$R_n^+ + e \rightarrow A_n + H$	16.86	-945	[16]
$A_n^+ + C_2H_2 \rightarrow A_{n+2}^+$	14.75	-	[16]

^aRate constant: $k = A \exp(-E/RT)$, $\text{cm}^3 \text{mole}^{-1} \text{s}^{-1}$.

3. Computational procedure

Analysis of the mechanisms of PAHs growth was carried out on the basis of comparison of the calculated concentration curves with the experimental data on the example of a laminar, one-dimensional, premixed benzene flame with axial diffusion: $C/O = 0.80$, the gas velocity in the burner v is equal 0.42 m/sec at a temperature $T = 298$ K and pressure $p = 2.66$ kPa [15]. Since the considered PAHs components are high-molecular compounds, their diffusion coefficients are much lower than the corresponding values for the light components of the flame. Therefore, it may be suggested that the diffusion effects have weak influence on their concentration profiles and can be neglected. In this case, to describe the dynamics of the process of transformation of the PAHs components, we can use the approximation of the plug-flow reactor.

The concentration of PAHs particles in hydrocarbon flames is much smaller than the concentration of components with which they interact (C_6H_6 , C_2H_2 , H_2 molecules, H radicals, etc.). This gives the possibility of separating the kinetics of their growth and the combustion kinetics. The available experimental data contain enough information for the approximation of the concentration curves of the light components of the flame and its temperature profile, which removes the problem of numerical modeling of the combustion in the flow with account for the transfer processes, and in describing the transformation of PAHs particles makes it possible to restrict ourselves to the solution of the direct kinetic problem.

Figure 1 shows the temperature and concentrations of intermediate components of the flame benzene/oxygen ($C/O = 0.72$, the mass fraction of argon in the initial mixture is 30%, $v_{298\text{ K}} = 0.5$ m/sec, $p = 2.67$ kPa) used in analyzing of mechanisms of PAHs formation [20]. PAHs molecules or radicals with the same number n but with a different content of H atoms were considered as one component: A_n or R_n . In the numerical realization of the coagulation mechanism, the n value was varied from 5 to 90, and the m value was varied from n to 90 (see the corresponding reactions given in the Table).

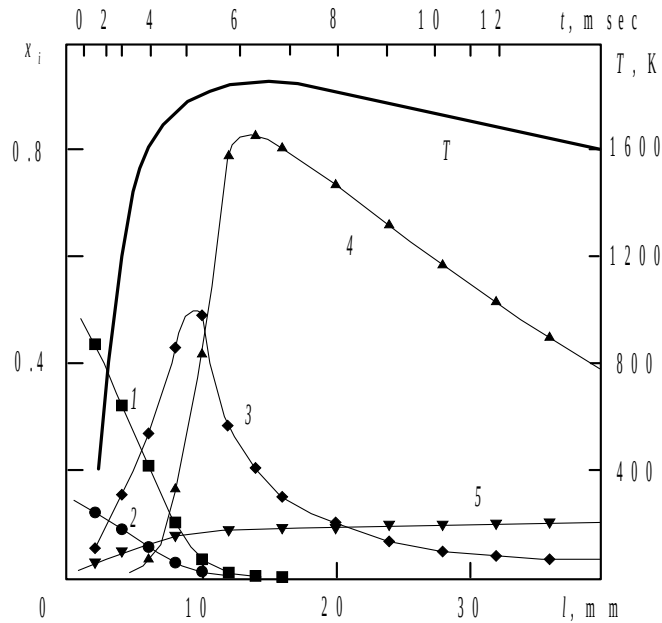


Figure 1: Molar fractions of components x_i (1-5) and temperature T (6) depending on the distance to the burner l and the process time t in the benzene/oxygen flame: 1) O_2 ; 2) C_6H_6 ; 3) C_2H_2 ($x_i \times 10$); 4) H ($x_i \times 10^2$); 5) H_2

4. Results and discussion

To estimate the contribution of different mechanisms to the formation dynamics of PAHs compounds, a series of calculations has been performed. The results of the calculation of maximum concentrations of PAHs molecules $(x_n)_{\max}$ with an even number of C atoms in a molecule are compared with the experimental data of [15] in Figure 2. As is seen, the HACA-mechanism (curve 1) gives a good agreement between calculated and measured concentrations $(x_n)_{\max}$ only at $n \leq 24$. The experimental values of $(x_n)_{\max}$ at $20 \leq n \leq 70$ remain at a level of about 10^{-6} , whereas the calculated values decrease sharply with increasing n . This can be due to the fact that in the considered flame at $l \geq 10$ mm there is a decrease in the concentration of C_2H_2 by more than an order of magnitude compared to its maximum value (see Figure 1), which in calculating by the HACA-mechanism leads to a corresponding decrease in the rate of formation of large aromatic molecules.

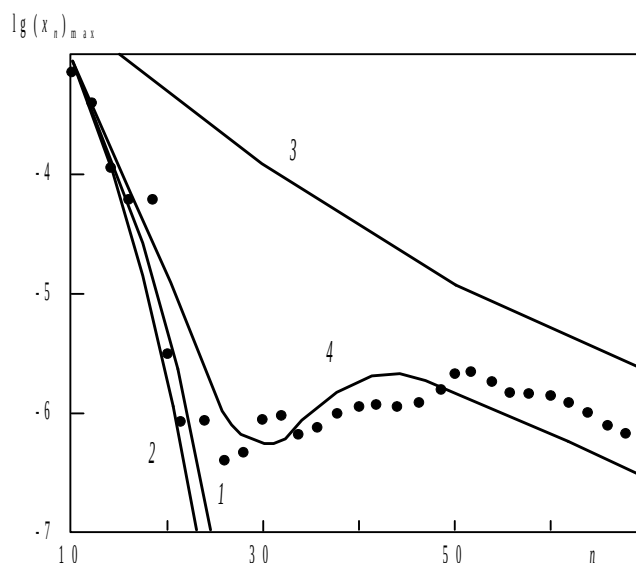


Figure 2: Maximum concentrations of PAHs molecules with an even number of C atoms as a function of n . Results of calculations: 1) HACA mechanism; 2) HACA mechanism + coagulation mechanism; 3) HACA mechanism + coagulation mechanism without account for inverse reactions; 4) recommended mechanism. Dots show the experimental data [15].

The growth of the aromatic structure of PAHs molecules in compliance with the HACA-mechanism presupposes a sequential increase in the mass of molecules under their interaction with acetylene molecules and, accordingly, a later appearance in the flame of heavy PAHs components. Nevertheless, the experimental data show that heavier PAHs molecules can appear in the flame at earlier stages of the process than light ones [21]. This indicates that the HACA-mechanism does not provide an adequate description of the process of formation of higher PAHs molecules in flame.

Including in consideration the coagulation mechanism leads to some decrease in concentrations $(x_n)_{\max}$ (see curve 2 in Figure 2). This somewhat unexpected result can be explained by the inverse reaction to the coagulation reaction: $A_{m+n} + H \rightarrow R_m + A_n$ (see the Table) that plays a dominant role in the formation and decomposition of biphenyl [13]. The interaction of two PAHs particles can lead, on the one hand, to the formation of biaryl (one C-C bond between two reagents), which then either decomposes into the initial components in the inverse reaction or, as a result of the internal restructuring, transforms into a more stable aromatic compound with the formation of a new ring. On the other hand, the *zipper* variety of the coagulation mechanism leads to appear of several C-C bonds between interacting PAHs particles simultaneously, which directly forms a stable aromatic molecule A_{m+n} without the formation of an intermediate biaryl compound. The interaction of this molecule with H-atom leads not to its decomposition into the initial components but to the formation of an aromatic radical in the reaction $A_{m+n} + H \rightarrow R_{m+n} + H_2$ (see HACA-mechanism in the Table). Nevertheless, an attempt to completely exclude the considered inverse reaction from the kinetic scheme gives values of the maximum concentration $(x_n)_{\max}$ in the range $20 \leq n \leq 70$ higher by one-two orders of magnitude (curve 3 in Figure 2).

The analysis performed makes it possible to distinguish the main features of the real formation mechanism of large PAHs molecules in benzene flames. This is, firstly, the ability of the HACA-mechanism to describe the behavior of aromatic components only for $n \leq 24$. Secondly, the coagulation mechanism in its irreversible form (*zipper*-mechanism) begins to work at $n \geq 20$. As mentioned above, the difference in reactivity between large PAHs radicals and molecules of equal structure at high temperatures is insignificant. Therefore, the kinetic model of the growth of the structure of PAHs particles with large n values should contain the coagulation of aromatic molecules with a rate constant equal to the corresponding value for the coagulation of aromatic radicals. As calculations show, the best agreement with

experimental data for the quantity $(x_n)_{\max}$ is reached, when the coagulation of aromatic molecules begins at $n \geq 16$.

Thus, the recommended formation mechanism of higher PAHs compounds in benzene flames includes the HACA-mechanism and the coagulation mechanism, in which decomposition of the molecule A_{m+n} under its interaction with H-atom occurs only at $m + n \leq 20$ and coagulation of aromatic molecules begins at $n = 16$. The results of the calculation on the basis of the given mechanism are presented by curve 4 in Figure 2. It is seen that in general the calculation data follow the behavior of the experimental points. In the range of large n values ($50 \leq n \leq 70$), the calculated values of the quantity $(x_n)_{\max}$ are about twice lower than the measured ones.

It should be noted that the PAHs components in the considered kinetic model differ only in the content of C-atoms without concrete definition of its internal structure and, accordingly, of the number of H-atoms. This imposes certain restrictions on the practical use of results obtained with the aid of the model. Nevertheless, the existing detailed kinetic models that consider in detail the growth of PAHs particles are unable to catch all essential details of the given process. In particular, the sufficiently comprehensive kinetic model developed in [22] gives a satisfactory agreement with experimental data only for compounds with $n \leq 20$.

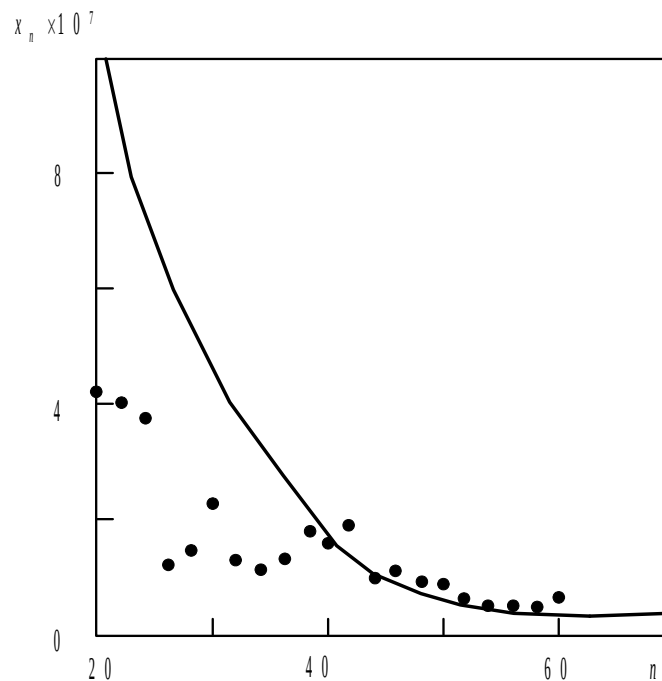


Figure 3: Concentration of PAHs molecules with an even number of C-atoms depending on n : dots show the experimental data [15] at $l = 7$ mm, the curve presents the results of calculations at $t = 5$ msec.

Figure 3 compares the results of calculations of the concentrations of PAHs molecules with an even number of C-atoms with the experimental data [15]. At the average, higher calculated data at $20 \leq n \leq 40$ and their lower values at $n > 40$ are observed, which agrees with the general trend of curve 4 in Figure 2. The behavior of the calculated dependences $x_n = x_n(t)$ follows the observed behavior of x_n along the jet axis. These values pass through the maximum within the limits of the fuel oxidation zone and then decrease so that in the combustion products the content of higher PAHs is insignificant. The distance l from the burner edge, at which the maximum of x_n is reached, increases, on average, with increasing n and is in the range $l = 9$ -12 mm, which agrees with the experimental data [15]. A typical profile of $x_n = x_n(t)$ is given in Figure 4.

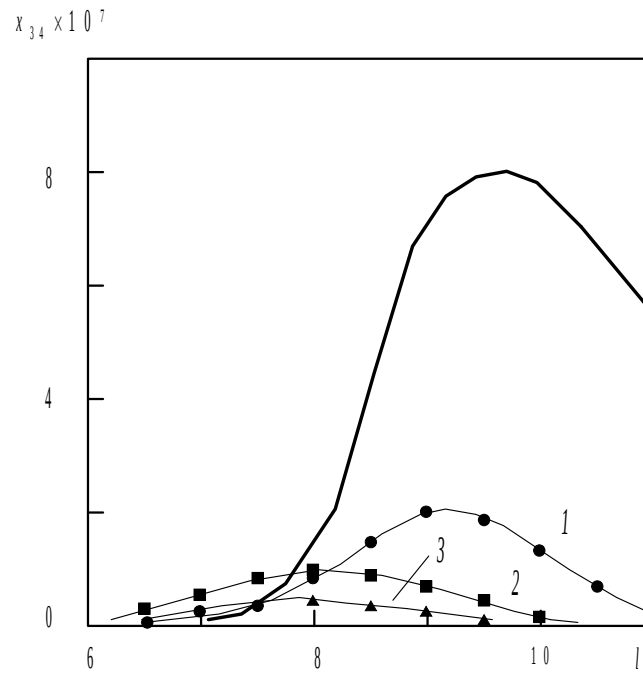


Figure 4: Concentration of C_{34} and its constituents depending on the distance l from the burner edge: dots show the experimental data [15]: 1 - $C_{34}H_{14}$; 2 - $C_{34}H_{16}$; 3 - $C_{34}H_{18}$; curve 4 presents the results of the calculation of the total concentration of C_{34} .

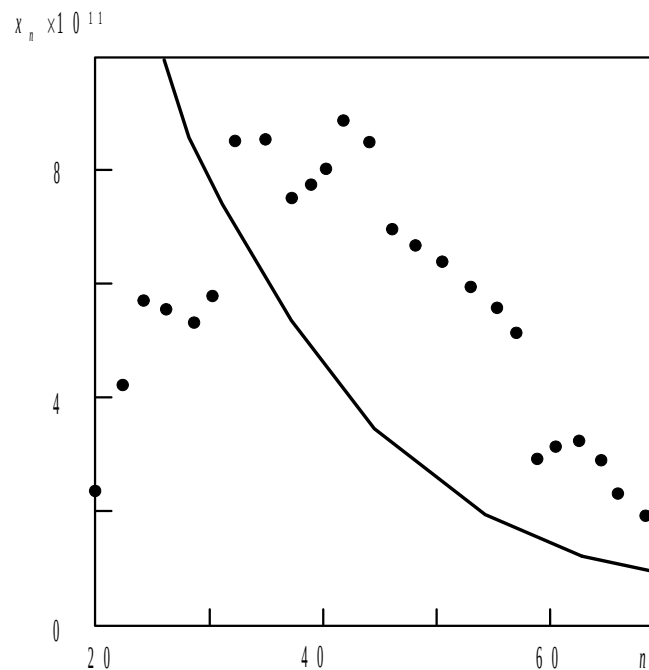


Figure 5: Concentrations of molecular ions PAH^+ with an even number of C-atoms depending on n : dots show the experimental data [24] at $l = 9$ mm; the curve presents the results of calculations at $t = 5.2$ msec.

The formation of aromatic ions PAH^+ was calculated at a given distribution of the H_3O^+ concentration along the jet axis [23] on the assumption that PAH^+ concentrations are much smaller than the concentration of H_3O^+ . The maximum value of the mole fraction of H_3O^+ reached at $l = 8$ mm was taken to be equal to 10^{-8} . Despite the fact that in the hydrocarbon flames the concentration maximum of negative ions is shifted relative to the maximum of positive ions towards the burner due to the diffusion effects [16], it is believed that the concentration of negative ions (electrons) at each instant of time is equal to the H_3O^+ concentrations.

The results of the calculation of concentrations of PAH^+ ions with an even number of C atoms are compared with the experimental data [24] in Figure 5. The calculation curve was obtained with the use of solely the mechanism of charge exchange of H_3O^+ on the corresponding PAHs molecules and subsequent recombination of PAH^+ and electrons. As is seen from the Table, the rate constant of the reaction of addition of C_2H_2 to the aromatic ion at $T = 2000$ K exceeds by two orders of magnitude the corresponding value for the addition of C_2H_2 to the PAHs radical. Therefore, the inclusion of the ion-molecular mechanism of PAH^+ growth in the computational algorithm leads to a fast equalization of PAH^+ concentrations at a level of $x_n(\text{PAH}^+) \approx 10^{-9}$. From this it follows that the given rate constant is at least one order of magnitude overstated.

5. Conclusions

The analysis of the existing mechanisms of higher PAHs formation in hydrocarbon flames makes it possible to distinguish the main features of the real formation mechanism. This is, firstly, the ability of the HACA-mechanism to describe the behavior of PAHs components only when a number n of C-atoms in aromatic molecule is less than 24. Secondly, the coagulation mechanism in its irreversible form (*zipper*-mechanism) begins to work at $n \geq 20$. Since the difference in reactivity between large PAHs radicals and molecules of equal structure at high temperatures is insignificant, then the kinetic model of the growth of the structure of PAHs molecules with large n values should contain the coagulation of aromatic molecules with a rate constant equal to the corresponding value for the coagulation of aromatic radicals. As calculations show, the best agreement with experimental data for the maximum concentrations of PAHs molecules in the flame is reached, when the coagulation mechanism of aromatic molecules growth begins to work at $n \geq 16$.

Results of this study can be useful for the prediction of PAHs and soot particles emission into the atmosphere from various combustion devices. Among them liquid-fuel rocket motors working on hydrocarbon fuels attract the special attention because harmful admixtures formed at rocket flights in the atmosphere are the only immediate anthropogenic pollutants at high altitudes.

References

- [1] McEnally, C. S., L. D. Pfefferle, B. Atakan, and K. Kohse-Hoinghaus. 2006. Studies of aromatic hydrocarbon formation mechanisms in flames: Progress towards closing the fuel gap. *Prog. Energy Combust. Sci.* 32:247-294.
- [2] Tishin, A. P., E. L. Alexandrov, A. V. Rodionov, et al. 1993. Impact of rocket flights on Earth ozone layer. *Chem. Phys.* 12:1184-1225.
- [3] Ross, M. 1996. Local effects of solid rocket motor exhaust on stratospheric ozone. *J. Spacecraft Rockets.* 33: 144-153.
- [4] Agafonov, G. L., I. Naydenova, P. A. Vlasov, and J. Warnatz. 2007. Detailed kinetic modelling of soot formation in shock tube pyrolysis and oxidation of toluene and *n*-heptane. *Proc. Combust. Inst.* 31:575-583.
- [5] Richter, H., and J. B. Howard. 2000. Formation of polycyclic aromatic hydrocarbons and their growth to soot - a review of chemical reaction pathways. *Prog. Energy Combust. Sci.* 26:565-608.
- [6] Gerasimov, G. Ya., and S. A. Losev. 2005. Kinetic models of combustion of kerosene and its components. *J. Eng. Phys. Thermophys.* 78:1059-1070.
- [7] Curran, H. J., P. Gaffuri, W. J. Pitz, and C. K. Westbrook. 1998. A comprehensive modeling study of *n*-heptane oxidation. *Combust. Flame.* 114:149-177.

- [8] Granata, S., T. Faravelli, and E. Ranzi. 2003. A wide range kinetic modeling study of the pyrolysis and combustion of naphthenes. *Combust. Flame*. 132:533-544.
- [9] Dagaut, P., G. Pengloan, and A. Ristory. 2002. Oxidation, ignition and combustion of toluene: Experimental and detailed chemical kinetic modeling. *Phys. Chem. Chem. Phys.* 4:1846-1854.
- [10] Wang, H., M. Frenklach. 1997. A detailed kinetic modelling study of aromatic formation in laminar premixed acetylene and ethylene flames. *Combust. Flame*. 110:173-221.
- [11] Rasmussen, C. L., M. S. Skjoth-Rasmussen, A. D. Jensen, P. Glarborg. 2005. Propargyl recombination: estimation of the high temperature, low pressure rate constant from flame measurements. *Proc. Combust. Inst.* 30:1023-1031.
- [12] Frenklach, M. 2002. Reaction mechanism of soot formation in flames. *Phys. Chem. Chem. Phys.* 4:2028-2037.
- [13] Park, J., and M. C. Lin. 1997. Kinetics for the recombination of phenyl radicals. *J. Phys. Chem.* A101:14-18.
- [14] Richter, H., S. Granata, W. H. Green, and J. B. Howard. 2005. Detailed modelling of PAH and soot formation in laminar premixed benzene/oxygen/argon low-pressure flame. *Proc. Combust. Inst.* 30:1397-1405.
- [15] Keller, A., R. Kovacs, and K.-H. Homann. 2000. Large molecules, ions, radicals and small soot particles in fuel-rich hydrocarbon flames. *Phys. Chem. Chem. Phys.* 2:1667-1675.
- [16] Fialkov, A. B. 1997. Investigation on ions in flames. *Prog. Energy Combust. Sci.* 23:399-528.
- [17] Lui, S., F. Jarrold, and M. T. Bowers. 1985. Ion-molecule clustering in simple systems. A study of the temperature dependence of the dimerization reactions of CH_2CF_2^+ , C_6H_6^+ (benzene), and C_6D_6^+ (benzene-*d*₆) in the parent neutral gases: experiment and theory. *J. Phys. Chem.* 89: 3127-3134.
- [18] Heckmann, E., H. Hipper, and J. Troe. 1996. High-temperature reactions and thermodynamic properties of phenyl radicals. *Proc. Combust. Inst.* 26:543-550.
- [19] Devis, S. G., H. Wang, K. Brezinsky, and C. K. Law. 1996. Laminar flame speeds and oxidation kinetics of benzene-air and toluene-air flames. *Proc. Combust. Inst.* 26:1025-1033.
- [20] Bittner, J. D., J. B. Howard, and H. B. Palmer. 1983. Chemistry of intermediate species in the rich combustion of benzene. In: J. Lahaye and G. Prado (Eds.), *Soot in Combustion Systems and Its Toxic Properties*. Plenum Press, New York. 95-125.
- [21] Hepp, H., K. Siegmann, and K. Sattler. 1995. New aspects of growth mechanisms for polycyclic aromatic hydrocarbons in diffusion flames. *Chem. Phys. Lett.* 233:16-22.
- [22] Richter, H., W. J. Grieco, and J. B. Howard. 1999. Formation mechanism of polycyclic aromatic hydrocarbons and fullerenes in premixed benzene flames. *Combust. Flame*. 119:1-22.
- [23] Prager, J., U. Riedel, and J. Warnatz. 2007. Modeling ion chemistry and charged species diffusion in lean methane-oxygen flames. *Proc. Combust. Inst.* 31:1129-1137.
- [24] Fialkov, A. B., J. Dennebaum, and K.-H. Homann. 2001. Large molecules, ions, radicals and small soot particles in fuel-rich hydrocarbon flames. Pt. V. Positive ions of polycyclic aromatic hydrocarbons (PAH) in low-pressure premixed flames of benzene and oxygen. *Combust. Flame*. 125:763-777.